REMCOM

XFdtd Validation for IEC/IEEE P62704-1\D4

Standard for Determining the Peak Spatial-Average Specific Absorption Rate (SAR) in the Human Body from Wireless Communication Devices, 30 MHz –6 GHz. Part 1: General requirements for using the Finite-Difference Time-Domain (FDTD) method for SAR calculations. 2016.

Contents

Overview

XFdtd 7.6.0 is compliant with and passes all tests outlined in the international Specific Absorption Rate (SAR) standards determined by the International Electrotechnical Commission (IEC) and the Institute of Electrical and Electronics Engineers (IEEE). The latest standard, including full problem descriptions, is detailed in the IEC draft [1].

The validation tests described in the standard are summarized below, presented with references to the corresponding IEC draft section, and followed by XFdtd's results.

Code Accuracy (IEC Section 8.2)

Several test problems are presented in the draft standard for the validation of FDTD code accuracy. Those tests and their results using XFdtd are described in this section.

Free Space Characteristics (IEC Section 8.2.1)

A quasi two-dimensional waveguide was used to determine the code's accuracy in wave propagation. The waveguide was excited by a broadband source and field values were used at several sample locations in conjunction with equations

provided in the standard. This determined the wave number and thus the accuracy of the Yee implementation of the software. The tests were for three waveguide fillings (free space, lossless dielectric, and lossy dielectric), two wave modes (transverse electric and transverse magnetic), and two grid definitions (homogeneous and inhomogeneous with the grid line locations provided in the standard). Additionally, the tests were performed for the waveguides oriented along the three axes of the coordinate system, for two different orientations around its axis (rotating the waveguide by 90°), and positive and negative propagation directions along the respective axis. The results of the 12 orientations must meet the minimum standards of +/- 2% for the homogenous cases and +/- 10% for the inhomogeneous cases when compared with analytical results. XFdtd's results are summarized in Tables 1–12 below.

	Limit for code compliance	**TE**			**TM**		
axis, direction of propagation and orientation	Z, +Z, XY						
ϵ_r		1	2	2	1	2	2
σ [S\m]		0	0	0.2	0	0	0.2
numerical f_{cutoff} [MHz]		1247	882	n.a.	1247	882	n.a.
max. dev. of simulated $Re\{k_z\}$ from numerical reference homogeneous mesh	$\pm$ 2 %	4.00E-01	4.40E-01	7.57E-02	3.46E-01	1.69E+00	7.57E-02
max. dev. of simulated $Im\{k_z\}$ from numerical reference homogeneous mesh	$\pm$ 2 %	n. a.	n. a.	4.12E-01	n. a.	n. a.	4.12E-01
max. dev. of simulated $Re\{k_x\}$ from numerical reference homogeneous mesh	$\pm$ 2 %	8.99E-05	1.14E-04	1.34E-04	8.18E-02	5.28E-02	6.76E-04
max. dev. of simulated $Re\{k_z\}$ from physical solution inhomogeneous mesh	$\pm$ 10 %	1.16E+00	1.310682	3.66E-01	1.25E+00	4.37E+00	3.67E-01
max. dev. of simulated $Im\{k_z\}$ from physical solution inhomogeneous mesh	$\pm$ 10 %	n. a.	n. a.	2.36007	n. a.	n. a.	2.357655
max. dev. of simulated $Re\{k_x\}$ from physical solution inhomogeneous mesh	$\pm$ 10 %	7.29E-02	7.29E-02	7.30E-02	1.08E-01	1.00E-01	7.40E-02
NOTE 1 The maximum deviation of the numerical evaluation shall be evaluated over the entire simulated frequency range (500 MHz to 2 GHz). NOTE 2 The frequency range $\pm$ 5 % around the cut-off frequencies shall be excluded from the evaluation of the kz components. This does not apply to the waveguide filled with the lossy dielectric. NOTE 3 The cut-off frequencies have been determined for the numerical waveguide model considering the numerical dispersion error. Therefore, they deviate from their physical values.							

Table 1: XFdtd's results of the numerical dispersion characteristics evaluation (IEC Table 6) for an XY orientation and +Z propagation direction.

	Limit for code compliance	**TE**			**TM**		
axis, direction of propagation and orientation	Z, -Z, XY						
ϵ_r		1	2	2	1	2	2
σ [S\m]		0	0	0.2	0	0	0.2
numerical f_{cutoff} [MHz]		1247	882	n.a.	1247	882	n.a.
max. dev. of simulated $Re\{k_z\}$ from numerical reference homogeneous mesh	± 2 %	4.00E-01	4.40E-01	7.57E-02	3.47E-01	1.69E+00	7.57E-02
max. dev. of simulated $Im\{k_z\}$ from numerical reference homogeneous mesh	± 2 %	n. a.	n. a.	4.12E-01	n. a.	n. a.	4.12E-01
max. dev. of simulated $Re\{k_x\}$ from numerical reference homogeneous mesh	± 2 %	8.99E-05	1.14E-04	1.34E-04	8.18E-02	5.28E-02	6.76E-04
max. dev. of simulated $Re\{k_z\}$ from physical solution inhomogeneous mesh	± 10 %	1.15933	1.310682	3.67E-01	1.12E+00	2.974707	3.66E-01
max. dev. of simulated $Im\{k_z\}$ from physical solution inhomogeneous mesh	± 10 %	n. a.	n. a.	2.36205	n. a.	n. a.	2.36208
max. dev. of simulated $Re\{k_x\}$ from physical solution inhomogeneous mesh	± 10 %	7.29E-02	7.29E-02	7.29E-02	1.11E-01	9.85E-02	7.37E-02
NOTE 1 The maximum deviation of the numerical evaluation shall be evaluated over the entire simulated frequency range (500 MHz to 2 GHz). NOTE 2 The frequency range ± 5 % around the cut-off frequencies shall be excluded from the evaluation of the kz components. This does not apply to the waveguide filled with the lossy dielectric. NOTE 3 The cut-off frequencies have been determined for the numerical waveguide model considering the numerical dispersion error. Therefore, they deviate from their physical values.							

Table 2: XFdtd's results of the numerical dispersion characteristics evaluation (IEC Table 6) for an XY orientation and -Z propagation direction.

	Limit for code compliance	**TE**			**TM**		
axis, direction of propagation and orientation	Z, +Z, YX						
ϵ_r		1	2	2	1	2	2
σ [S\m]		0	0	0.2	0	0	0.2
numerical f_{cutoff} [MHz]		1247	882	n.a.	1247	882	n.a.
max. dev. of simulated $Re\{k_z\}$ from numerical reference homogeneous mesh	± 2 %	4.00E-01	4.40E-01	7.57E-02	3.45E-01	1.73E+00	7.57E-02
max. dev. of simulated $Im\{k_z\}$ from numerical reference homogeneous mesh	± 2 %	n. a.	n. a.	4.12E-01	n. a.	n. a.	4.12E-01
max. dev. of simulated $Re\{k_x\}$ from numerical reference homogeneous mesh	± 2 %	9.88E-05	1.22E-04	1.27E-04	5.77E-02	5.44E-02	5.55E-04
max. dev. of simulated $Re\{k_z\}$ from physical solution inhomogeneous mesh	± 10 %	1.159264	1.310759	3.66E-01	1.26E+00	4.362673	3.68E-01
max. dev. of simulated $Im\{k_z\}$ from physical solution inhomogeneous mesh	± 10 %	n. a.	n. a.	2.36006	n. a.	n. a.	2.357395
max. dev. of simulated $Re\{k_x\}$ from physical solution inhomogeneous mesh	± 10 %	7.29E-02	7.29E-02	7.30E-02	1.33E-01	1.74E-01	7.42E-02
NOTE 1 The maximum deviation of the numerical evaluation shall be evaluated over the entire simulated frequency range (500 MHz to 2 GHz). NOTE 2 The frequency range ± 5 % around the cut-off frequencies shall be excluded from the evaluation of the kz components. This does not apply to the waveguide filled with the lossy dielectric. NOTE 3 The cut-off frequencies have been determined for the numerical waveguide model considering the numerical dispersion error. Therefore, they deviate from their physical values.							

Table 3: XFdtd's results of the numerical dispersion characteristics evaluation (IEC Table 6) for an YX orientation and +Z propagation direction.

	Limit for code compliance	**TE**			**TM**		
axis, direction of propagation and orientation	Z, -Z, YX						
ϵ_r		1	2	2	1	2	2
σ [S\m]		0	0	0.2	0	0	0.2
numerical f_{cutoff} [MHz]		1247	882	n.a.	1247	882	n.a.
max. dev. of simulated $Re\{k_z\}$ from numerical reference homogeneous mesh	± 2 %	4.00E-01	4.40E-01	7.57E-02	3.45E-01	1.73E+00	7.57E-02
max. dev. of simulated $Im\{k_z\}$ from numerical reference homogeneous mesh	± 2 %	n. a.	n. a.	4.12E-01	n. a.	n. a.	4.12E-01
max. dev. of simulated $Re\{k_x\}$ from numerical reference homogeneous mesh	± 2 %	9.88E-05	1.22E-04	1.27E-04	5.77E-02	5.44E-02	5.55E-04
max. dev. of simulated $Re\{k_z\}$ from physical solution inhomogeneous mesh	± 10 %	1.159264	1.310759	3.66E-01	1.71E+00	3.009202	3.66E-01
max. dev. of simulated $Im\{k_z\}$ from physical solution inhomogeneous mesh	± 10 %	n. a.	n. a.	2.36006	n. a.	n. a.	2.361808
max. dev. of simulated $Re\{k_x\}$ from physical solution inhomogeneous mesh	± 10 %	7.29E-02	7.29E-02	7.30E-02	1.10E-01	1.34E-01	7.39E-02
NOTE 1 The maximum deviation of the numerical evaluation shall be evaluated over the entire simulated frequency range (500 MHz to 2 GHz). NOTE 2 The frequency range ± 5 % around the cut-off frequencies shall be excluded from the evaluation of the kz components. This does not apply to the waveguide filled with the lossy dielectric. NOTE 3 The cut-off frequencies have been determined for the numerical waveguide model considering the numerical dispersion error. Therefore, they deviate from their physical values.							

Table 4: XFdtd's results of the numerical dispersion characteristics evaluation (IEC Table 6) for an YX orientation and -Z propagation direction.

	Limit for code compliance	**TE**			**TM**		
axis, direction of propagation and orientation	X, +X, YZ						
ϵ_r		1	2	2	1	2	2
σ [S\m]		0	0	0.2	0	0	0.2
numerical f_{cutoff} [MHz]		1247	882	n.a.	1247	882	n.a.
max. dev. of simulated $Re\{k_z\}$ from numerical reference homogeneous mesh	± 2 %	4.00E-01	4.40E-01	7.57E-02	3.46E-01	1.78E+00	7.57E-02
max. dev. of simulated $Im\{k_z\}$ from numerical reference homogeneous mesh	± 2 %	n. a.	n. a.	4.12E-01	n. a.	n. a.	4.12E-01
max. dev. of simulated $Re\{k_x\}$ from numerical reference homogeneous mesh	± 2 %	8.99E-05	1.52E-04	1.16E-04	8.18E-02	6.61E-02	5.55E-04
max. dev. of simulated $Re\{k_z\}$ from physical solution inhomogeneous mesh	± 10 %	1.16E+00	1.310785	3.66E-01	1.26E+00	4.236622	3.67E-01
max. dev. of simulated $Im\{k_z\}$ from physical solution inhomogeneous mesh	± 10 %	n. a.	n. a.	2.360109	n. a.	n. a.	2.357631
max. dev. of simulated $Re\{k_x\}$ from physical solution inhomogeneous mesh	± 10 %	7.29E-02	7.30E-02	7.30E-02	9.16E-02	1.13E-01	7.33E-02
NOTE 1 The maximum deviation of the numerical evaluation shall be evaluated over the entire simulated frequency range (500 MHz to 2 GHz). NOTE 2 The frequency range ± 5 % around the cut-off frequencies shall be excluded from the evaluation of the kz components. This does not apply to the waveguide filled with the lossy dielectric. NOTE 3 The cut-off frequencies have been determined for the numerical waveguide model considering the numerical dispersion error. Therefore, they deviate from their physical values.							

Table 5: XFdtd's results of the numerical dispersion characteristics evaluation (IEC Table 6) for an YZ orientation and +X propagation direction.

	Limit for code compliance	**TE**			**TM**		
axis, direction of propagation and orientation	X, -X, YZ						
ϵ_r		1	2	2	1	2	2
σ [S\m]		0	0	0.2	0	0	0.2
numerical f_{cutoff} [MHz]		1247	882	n.a.	1247	882	n.a.
max. dev. of simulated $Re\{k_z\}$ from numerical reference homogeneous mesh	$\pm$ 2 %	4.00E-01	4.40E-01	7.57E-02	3.55E-01	1.78E+00	7.57E-02
max. dev. of simulated $Im\{k_z\}$ from numerical reference homogeneous mesh	$\pm$ 2 %	n. a.	n. a.	4.12E-01	n. a.	n. a.	4.12E-01
max. dev. of simulated $Re\{k_x\}$ from numerical reference homogeneous mesh	$\pm$ 2 %	7.87E-05	1.52E-04	1.16E-04	1.07E-01	6.61E-02	5.55E-04
max. dev. of simulated $Re\{k_z\}$ from physical solution inhomogeneous mesh	$\pm$ 10 %	1.159292	1.310785	3.66E-01	1.67E+00	2.892055	3.67E-01
max. dev. of simulated $Im\{k_z\}$ from physical solution inhomogeneous mesh	$\pm$ 10 %	n. a.	n. a.	2.360109	n. a.	n. a.	2.361958
max. dev. of simulated $Re\{k_x\}$ from physical solution inhomogeneous mesh	$\pm$ 10 %	7.29E-02	7.30E-02	7.30E-02	9.30E-02	9.17E-02	7.33E-02
NOTE 1 The maximum deviation of the numerical evaluation shall be evaluated over the entire simulated frequency range (500 MHz to 2 GHz). NOTE 2 The frequency range $\pm$ 5 % around the cut-off frequencies shall be excluded from the evaluation of the kz components. This does not apply to the waveguide filled with the lossy dielectric. NOTE 3 The cut-off frequencies have been determined for the numerical waveguide model considering the numerical dispersion error. Therefore, they deviate from their physical values.							

Table 6: XFdtd's results of the numerical dispersion characteristics evaluation (IEC Table 6) for an YZ orientation and -X propagation direction.

	Limit for code compliance	**TE**			**TM**		
axis, direction of propagation and orientation	X, +X, ZY						
ϵ_r		1	2	2	1	2	2
σ [S\m]		0	0	0.2	0	0	0.2
numerical f_{cutoff} [MHz]		1247	882	n.a.	1247	882	n.a.
max. dev. of simulated $Re\{k_z\}$ from numerical reference homogeneous mesh	$\pm$ 2 %	4.00E-01	4.40E-01	7.57E-02	3.20E-01	1.76E+00	7.57E-02
max. dev. of simulated $Im\{k_z\}$ from numerical reference homogeneous mesh	$\pm$ 2 %	n. a.	n. a.	4.12E-01	n. a.	n. a.	4.12E-01
max. dev. of simulated $Re\{k_x\}$ from numerical reference homogeneous mesh	$\pm$ 2 %	1.29E-04	1.62E-04	1.10E-04	8.01E-02	6.66E-02	5.09E-04
max. dev. of simulated $Re\{k_z\}$ from physical solution inhomogeneous mesh	$\pm$ 10 %	1.159171	1.310649	3.66E-01	1.29E+00	4.417289	3.68E-01
max. dev. of simulated $Im\{k_z\}$ from physical solution inhomogeneous mesh	$\pm$ 10 %	n. a.	n. a.	2.360152	n. a.	n. a.	2.357713
max. dev. of simulated $Re\{k_x\}$ from physical solution inhomogeneous mesh	$\pm$ 10 %	7.29E-02	7.29E-02	7.30E-04	1.43E-01	1.46E-01	7.33E-02
NOTE 1 The maximum deviation of the numerical evaluation shall be evaluated over the entire simulated frequency range (500 MHz to 2 GHz). NOTE 2 The frequency range $\pm$ 5 % around the cut-off frequencies shall be excluded from the evaluation of the kz components. This does not apply to the waveguide filled with the lossy dielectric. NOTE 3 The cut-off frequencies have been determined for the numerical waveguide model considering the numerical dispersion error. Therefore, they deviate from their physical values.							

Table 7: XFdtd's results of the numerical dispersion characteristics evaluation (IEC Table 6) for an ZY orientation and +X propagation direction.

	Limit for code compliance	**TE**			**TM**		
axis, direction of propagation and orientation	X, -X, ZY						
ϵ_r		1	2	2	1	2	2
σ [S\m]		0	0	0.2	0	0	0.2
numerical f_{cutoff} [MHz]		1247	882	n.a.	1247	882	n.a.
max. dev. of simulated $Re\{k_z\}$ from numerical reference homogeneous mesh	$\pm$ 2 %	4.00E-01	4.40E-01	7.57E-02	3.20E-01	1.76E+00	7.57E-02
max. dev. of simulated $Im\{k_z\}$ from numerical reference homogeneous mesh	$\pm$ 2 %	n. a.	n. a.	4.12E-01	n. a.	n. a.	4.12E-01
max. dev. of simulated $Re\{k_x\}$ from numerical reference homogeneous mesh	$\pm$ 2 %	1.29E-04	1.62E-04	1.10E-04	8.01E-02	6.66E-02	5.09E-04
max. dev. of simulated $Re\{k_z\}$ from physical solution inhomogeneous mesh	$\pm$ 10 %	1.159171	1.310649	3.66E-01	1.73E+00	3.000909	3.66E-01
max. dev. of simulated $Im\{k_z\}$ from physical solution inhomogeneous mesh	$\pm$ 10 %	n. a.	n. a.	2.360152	n. a.	n. a.	2.361882
max. dev. of simulated $Re\{k_x\}$ from physical solution inhomogeneous mesh	$\pm$ 10 %	7.29E-02	7.29E-02	7.30E-02	1.33E-01	1.27E-01	7.34E-02
NOTE 1 The maximum deviation of the numerical evaluation shall be evaluated over the entire simulated frequency range (500 MHz to 2 GHz). NOTE 2 The frequency range $\pm$ 5 % around the cut-off frequencies shall be excluded from the evaluation of the kz components. This does not apply to the waveguide filled with the lossy dielectric. NOTE 3 The cut-off frequencies have been determined for the numerical waveguide model considering the numerical dispersion error. Therefore, they deviate from their physical values.							

Table 8: XFdtd's results of the numerical dispersion characteristics evaluation (IEC Table 6) for an ZY orientation and -X propagation direction.

	Limit for code compliance	**TE**			**TM**		
axis, direction of propagation and orientation	Y, +Y, XZ						
ϵ_r		1	2	2	1	2	2
σ [S\m]		0	0	0.2	0	0	0.2
numerical f_{cutoff} [MHz]		1247	882	n.a.	1247	882	n.a.
max. dev. of simulated $Re\{k_z\}$ from numerical reference homogeneous mesh	± 2 %	4.00E-01	4.40E-01	7.57E-02	3.20E-01	1.76E+00	7.57E-02
max. dev. of simulated $Im\{k_z\}$ from numerical reference homogeneous mesh	± 2 %	n. a.	n. a.	4.12E-01	n. a.	n. a.	4.12E-01
max. dev. of simulated $Re\{k_x\}$ from numerical reference homogeneous mesh	± 2 %	1.29E-04	1.62E-04	1.10E-04	8.01E-02	6.66E-02	5.09E-04
max. dev. of simulated $Re\{k_z\}$ from physical solution inhomogeneous mesh	± 10 %	1.16E+00	1.310649	3.66E-01	1.29E+00	4.417289	3.68E-01
max. dev. of simulated $Im\{k_z\}$ from physical solution inhomogeneous mesh	± 10 %	n. a.	n. a.	2.360152	n. a.	n. a.	2.357713
max. dev. of simulated $Re\{k_x\}$ from physical solution inhomogeneous mesh	± 10 %	7.29E-02	7.29E-02	7.30E-02	1.43E-01	1.46E-01	7.33E-02
NOTE 1 The maximum deviation of the numerical evaluation shall be evaluated over the entire simulated frequency range (500 MHz to 2 GHz). NOTE 2 The frequency range ± 5 % around the cut-off frequencies shall be excluded from the evaluation of the kz components. This does not apply to the waveguide filled with the lossy dielectric. NOTE 3 The cut-off frequencies have been determined for the numerical waveguide model considering the numerical dispersion error. Therefore, they deviate from their physical values.							

Table 9: XFdtd's results of the numerical dispersion characteristics evaluation (IEC Table 6) for an XZ orientation and +Y propagation direction.

	Limit for code compliance	**TE**			**TM**		
axis, direction of propagation and orientation	Y, -Y, XZ						
ϵ_r		1	2	2	1	2	2
σ [S\m]		0	0	0.2	0	0	0.2
numerical f_{cutoff} [MHz]		1247	882	n.a.	1247	882	n.a.
max. dev. of simulated $Re\{k_z\}$ from numerical reference homogeneous mesh	$\pm$ 2 %	4.00E-01	4.40E-01	7.57E-02	3.20E-01	1.76E+00	7.57E-02
max. dev. of simulated $Im\{k_z\}$ from numerical reference homogeneous mesh	$\pm$ 2 %	n. a.	n. a.	4.12E-01	n. a.	n. a.	4.12E-01
max. dev. of simulated $Re\{k_x\}$ from numerical reference homogeneous mesh	$\pm$ 2 %	1.29E-04	1.62E-04	1.10E-04	8.01E-02	6.66E-02	5.09E-04
max. dev. of simulated $Re\{k_z\}$ from physical solution inhomogeneous mesh	$\pm$ 10 %	1.159171	1.310649	3.66E-01	1.73E+00	3.000909	3.66E-01
max. dev. of simulated $Im\{k_z\}$ from physical solution inhomogeneous mesh	$\pm$ 10 %	n. a.	n. a.	2.360152	n. a.	n. a.	2.361882
max. dev. of simulated $Re\{k_x\}$ from physical solution inhomogeneous mesh	$\pm$ 10 %	7.29E-02	7.29E-02	7.30E-02	1.33E-01	1.27E-01	7.34E-02
NOTE 1 The maximum deviation of the numerical evaluation shall be evaluated over the entire simulated frequency range (500 MHz to 2 GHz). NOTE 2 The frequency range $\pm$ 5 % around the cut-off frequencies shall be excluded from the evaluation of the kz components. This does not apply to the waveguide filled with the lossy dielectric. NOTE 3 The cut-off frequencies have been determined for the numerical waveguide model considering the numerical dispersion error. Therefore, they deviate from their physical values.							

Table 10: XFdtd's results of the numerical dispersion characteristics evaluation (IEC Table 6) for an XZ orientation and -Y propagation direction.

	Limit for code compliance	**TE**			**TM**		
axis, direction of propagation and orientation	Y, +Y, ZX						
ϵ_r		1	2	2	1	2	2
σ [S\m]		0	0	0.2	0	0	0.2
numerical f_{cutoff} [MHz]		1247	882	n.a.	1247	882	n.a.
max. dev. of simulated $Re\{k_z\}$ from numerical reference homogeneous mesh	± 2 %	4.00E-01	4.40E-01	7.57E-02	3.55E-01	1.78E+00	7.57E-02
max. dev. of simulated $Im\{k_z\}$ from numerical reference homogeneous mesh	± 2 %	n. a.	n. a.	4.12E-01	n. a.	n. a.	4.12E-01
max. dev. of simulated $Re\{k_x\}$ from numerical reference homogeneous mesh	± 2 %	7.87E-05	1.52E-04	1.16E-04	1.07E-01	6.61E-02	5.55E-04
max. dev. of simulated $Re\{k_z\}$ from physical solution inhomogeneous mesh	± 10 %	1.159292	1.310785	3.66E-01	1.26E+00	4.236622	3.67E-01
max. dev. of simulated $Im\{k_z\}$ from physical solution inhomogeneous mesh	± 10 %	n. a.	n. a.	2.360109	n. a.	n. a.	2.357631
max. dev. of simulated $Re\{k_x\}$ from physical solution inhomogeneous mesh	± 10 %	7.29E-02	7.30E-02	7.30E-02	9.16E-02	1.13E-01	7.33E-02
NOTE 1 The maximum deviation of the numerical evaluation shall be evaluated over the entire simulated frequency range (500 MHz to 2 GHz). NOTE 2 The frequency range ± 5 % around the cut-off frequencies shall be excluded from the evaluation of the kz components. This does not apply to the waveguide filled with the lossy dielectric. NOTE 3 The cut-off frequencies have been determined for the numerical waveguide model considering the numerical dispersion error. Therefore, they deviate from their physical values.							

Table 11: XFdtd's results of the numerical dispersion characteristics evaluation (IEC Table 6) for an ZX orientation and +Y propagation direction.

	Limit for code compliance	**TE**			**TM**		
axis, direction of propagation and orientation	Y, -Y, ZX						
ϵ_r		1	2	2	1	2	2
σ [S\m]		0	0	0.2	0	0	0.2
numerical f_{cutoff} [MHz]		1247	882	n.a.	1247	882	n.a.
max. dev. of simulated $Re\{k_z\}$ from numerical reference homogeneous mesh	$\pm$ 2 %	4.00E-01	4.40E-01	7.57E-02	3.55E-01	1.78E+00	7.57E-02
max. dev. of simulated $Im\{k_z\}$ from numerical reference homogeneous mesh	$\pm$ 2 %	n. a.	n. a.	4.12E-01	n. a.	n. a.	4.12E-01
max. dev. of simulated $Re\{k_x\}$ from numerical reference homogeneous mesh	$\pm$ 2 %	7.87E-05	1.52E-04	1.16E-04	1.07E-01	6.61E-02	5.55E-04
max. dev. of simulated $Re\{k_z\}$ from physical solution inhomogeneous mesh	$\pm$ 10 %	1.159292	1.310785	3.66E-01	1.67E+00	2.892055	3.67E-01
max. dev. of simulated $Im\{k_z\}$ from physical solution inhomogeneous mesh	$\pm$ 10 %	n. a.	n. a.	2.360109	n. a.	n. a.	2.361958
max. dev. of simulated $Re\{k_x\}$ from physical solution inhomogeneous mesh	$\pm$ 10 %	7.29E-02	7.30E-02	7.30E-02	9.30E-02	9.17E-02	7.33E-02
NOTE 1 The maximum deviation of the numerical evaluation shall be evaluated over the entire simulated frequency range (500 MHz to 2 GHz). NOTE 2 The frequency range $\pm$ 5 % around the cut-off frequencies shall be excluded from the evaluation of the kz components. This does not apply to the waveguide filled with the lossy dielectric. NOTE 3 The cut-off frequencies have been determined for the numerical waveguide model considering the numerical dispersion error. Therefore, they deviate from their physical values.							

Table 12: XFdtd's results of the numerical dispersion characteristics evaluation (IEC Table 6) for an ZX orientation and -Y propagation direction.

Planar Dielectric Boundaries (IEC Section 8.2.2)

The tests described in this section are similar to those in the Free Space Characteristics section, except that here only homogeneous grids are required, a free space/dielectric boundary was introduced to the waveguide, and the reflection coefficient was computed. Lossless and lossy dielectric materials were used for the TE cases, while only a lossless dielectric was used for the TM case. Additionally, results were evaluated and reported for the waveguide oriented along the three axes of the coordinate system, for two different orientations around its axis (rotating the waveguide by 90°), and positive and negative propagation directions along the respective axis. XFdtd's results for the 12 orientations are shown in Tables 13–24.

	Limit for code compliance	**TE**		**TM**
axis, direction of propagation and orientation	Z, +Z, XY			
ϵ_r		4	4	4
σ [S\m]		0	0.2	0
max. dev. of simulated $Re\{k_{2z}\}$ from numerical reference 1.3 GHz $<$ f $<$ 2 GHz	± 5,0 %	4.76E-03	2.51E-02	1.37E-03
max. dev. of simulated $Im\{k_{2z}\}$ from numerical reference 0.5 GHz $<$ f $<$ 0.6 GHz	± 5,0 %	n. a.	2.12E-02	n. a.
max. dev. of simulated $Re\{r\}$ from numerical reference 1.3 GHz $<$ f $<$ 2 GHz	± 5,0 %	4.95E-03	4.92E-04	3.14E-01
max. dev. of simulated $Im\{r\}$ from numerical reference 1.3 GHz $<$ f $<$ 2 GHz	± 5,0 %	n. a.	1.60E-03	n. a.
max. dev. of simulated $Re\{r\}$ from numerical reference 0.5 GHz $<$ f $<$ 0.6 GHz	± 10,0 %	3.53E-01	4.16E-02	1.12E-01
max. dev. of simulated $Im\{r\}$ from numerical reference 0.5 GHz $<$ f $<$ 0.6 GHz	± 10,0 %	n. a.	3.94E-02	n. a.
The frequency range is indicated for each value to be reported. NOTE Larger tolerances apply for the deviation of the simulation from the reference for frequencies between 0.5 GHz and 0.6 GHz (below cut-off).				

Table 13: XFdtd's results of numerical reflection coefficient evaluation (IEC Table 7) for an XY orientation and +Z propagation direction.

	Limit for code compliance	**TE**		**TM**
axis, direction of propagation and orientation	Z, -Z, XY			
ϵ_r		4	4	4
σ [S\m]		0	0.2	0
max. dev. of simulated $Re\{k_{2z}\}$ from numerical reference 1.3 GHz $<$ f $<$ 2 GHz	$\pm$ 5,0 %	4.76E-03	2.51E-02	1.29E-03
max. dev. of simulated $Im\{k_{2z}\}$ from numerical reference 0.5 GHz $<$ f $<$ 0.6 GHz	$\pm$ 5,0 %	n. a.	2.12E-02	n. a.
max. dev. of simulated $Re\{r\}$ from numerical reference 1.3 GHz $<$ f $<$ 2 GHz	$\pm$ 5,0 %	4.95E-03	4.92E-04	2.72E-01
max. dev. of simulated $Im\{r\}$ from numerical reference 1.3 GHz $<$ f $<$ 2 GHz	$\pm$ 5,0 %	n. a.	1.60E-03	n. a.
max. dev. of simulated $Re\{r\}$ from numerical reference 0.5 GHz $<$ f $<$ 0.6 GHz	$\pm$ 10,0 %	3.53E-01	4.16E-02	1.15E-01
max. dev. of simulated $Im\{r\}$ from numerical reference 0.5 GHz $<$ f $<$ 0.6 GHz	$\pm$ 10,0 %	n. a.	3.94E-02	n. a.
The frequency range is indicated for each value to be reported. NOTE Larger tolerances apply for the deviation of the simulation from the reference for frequencies between 0.5 GHz and 0.6 GHz (below cut-off).				

Table 14: XFdtd's results of numerical reflection coefficient evaluation (IEC Table 7) for an XY orientation and -Z propagation direction.

	Limit for code compliance	**TE**		**TM**
axis, direction of propagation and orientation	Z, +Z, YX			
ϵ_r		4	4	4
σ [S\m]		0	0.2	0
max. dev. of simulated $Re\{k_{2z}\}$ from numerical reference 1.3 GHz $<$ f $<$ 2 GHz	$\pm$ 5,0 %	4.91E-03	2.51E-02	9.09E-04
max. dev. of simulated $Im\{k_{2z}\}$ from numerical reference 0.5 GHz $<$ f $<$ 0.6 GHz	$\pm$ 5,0 %	n. a.	2.13E-02	n. a.
max. dev. of simulated $Re\{r\}$ from numerical reference 1.3 GHz $<$ f $<$ 2 GHz	$\pm$ 5,0 %	4.86E-03	6.90E-04	3.73E-01
max. dev. of simulated $Im\{r\}$ from numerical reference 1.3 GHz $<$ f $<$ 2 GHz	$\pm$ 5,0 %	n. a.	1.82E-03	n. a.
max. dev. of simulated $Re\{r\}$ from numerical reference 0.5 GHz $<$ f $<$ 0.6 GHz	$\pm$ 10,0 %	3.51E-01	4.69E-02	1.20E-01
max. dev. of simulated $Im\{r\}$ from numerical reference 0.5 GHz $<$ f $<$ 0.6 GHz	$\pm$ 10,0 %	n. a.	3.59E-02	n. a.
The frequency range is indicated for each value to be reported. NOTE Larger tolerances apply for the deviation of the simulation from the reference for frequencies between 0.5 GHz and 0.6 GHz (below cut-off).				

Table 15: XFdtd's results of numerical reflection coefficient evaluation (IEC Table 7) for an YX orientation and +Z propagation direction.

	Limit for code compliance	**TE**		**TM**
axis, direction of propagation and orientation	Z, -Z, YX			
ϵ_r		4	4	4
σ [S\m]		0	0.2	0
max. dev. of simulated $Re\{k_{2z}\}$ from numerical reference 1.3 GHz $<$ f $<$ 2 GHz	$\pm$ 5,0 %	4.91E-03	2.51E-02	8.41E-04
max. dev. of simulated $Im\{k_{2z}\}$ from numerical reference 0.5 GHz $<$ f $<$ 0.6 GHz	$\pm$ 5,0 %	n. a.	2.13E-02	n. a.
max. dev. of simulated $Re\{r\}$ from numerical reference 1.3 GHz $<$ f $<$ 2 GHz	$\pm$ 5,0 %	4.86E-03	6.90E-04	3.80E-01
max. dev. of simulated $Im\{r\}$ from numerical reference 1.3 GHz $<$ f $<$ 2 GHz	$\pm$ 5,0 %	n. a.	1.82E-03	n. a.
max. dev. of simulated $Re\{r\}$ from numerical reference 0.5 GHz $<$ f $<$ 0.6 GHz	$\pm$ 10,0 %	3.51E-01	4.69E-02	1.15E-01
max. dev. of simulated $Im\{r\}$ from numerical reference 0.5 GHz $<$ f $<$ 0.6 GHz	$\pm$ 10,0 %	n. a.	3.59E-02	n. a.
The frequency range is indicated for each value to be reported. NOTE Larger tolerances apply for the deviation of the simulation from the reference for frequencies between 0.5 GHz and 0.6 GHz (below cut-off).				

Table 16: XFdtd's results of numerical reflection coefficient evaluation (IEC Table 7) for an YX orientation and -Z propagation direction.

	Limit for code compliance	**TE**		**TM**
axis, direction of propagation and orientation	X, +X, YZ			
ϵ_r		4	4	4
σ [S\m]		0	0.2	0
max. dev. of simulated $Re\{k_{2z}\}$ from numerical reference 1.3 GHz $<$ f $<$ 2 GHz	$\pm$ 5,0 %	4.76E-03	2.51E-02	1.37E-03
max. dev. of simulated $Im\{k_{2z}\}$ from numerical reference 0.5 GHz $<$ f $<$ 0.6 GHz	$\pm$ 5,0 %	n. a.	2.12E-02	n. a.
max. dev. of simulated $Re\{r\}$ from numerical reference 1.3 GHz $<$ f $<$ 2 GHz	$\pm$ 5,0 %	4.95E-03	4.92E-04	3.14E-01
max. dev. of simulated $Im\{r\}$ from numerical reference 1.3 GHz $<$ f $<$ 2 GHz	$\pm$ 5,0 %	n. a.	1.60E-03	n. a.
max. dev. of simulated $Re\{r\}$ from numerical reference 0.5 GHz $<$ f $<$ 0.6 GHz	$\pm$ 10,0 %	3.53E-01	4.16E-02	1.12E-01
max. dev. of simulated $Im\{r\}$ from numerical reference 0.5 GHz $<$ f $<$ 0.6 GHz	$\pm$ 10,0 %	n. a.	3.94E-02	n. a.
The frequency range is indicated for each value to be reported. NOTE Larger tolerances apply for the deviation of the simulation from the reference for frequencies between 0.5 GHz and 0.6 GHz (below cut-off).				

Table 17: XFdtd's results of numerical reflection coefficient evaluation (IEC Table 7) for an YZ orientation and +X propagation direction.

	Limit for code compliance	**TE**		**TM**
axis, direction of propagation and orientation	X, -X, YZ			
ϵ_r		4	4	4
σ [S\m]		0	0.2	0
max. dev. of simulated $Re\{k_{2z}\}$ from numerical reference 1.3 GHz $<$ f $<$ 2 GHz	$\pm$ 5,0 %	4.76E-03	2.51E-02	1.29E-03
max. dev. of simulated $Im\{k_{2z}\}$ from numerical reference 0.5 GHz $<$ f $<$ 0.6 GHz	$\pm$ 5,0 %	n. a.	2.12E-02	n. a.
max. dev. of simulated $Re\{r\}$ from numerical reference 1.3 GHz $<$ f $<$ 2 GHz	$\pm$ 5,0 %	4.95E-03	4.92E-04	2.72E-01
max. dev. of simulated $Im\{r\}$ from numerical reference 1.3 GHz $<$ f $<$ 2 GHz	$\pm$ 5,0 %	n. a.	1.60E-03	n. a.
max. dev. of simulated $Re\{r\}$ from numerical reference 0.5 GHz $<$ f $<$ 0.6 GHz	$\pm$ 10,0 %	3.53E-01	4.16E-02	1.15E-01
max. dev. of simulated $Im\{r\}$ from numerical reference 0.5 GHz $<$ f $<$ 0.6 GHz	$\pm$ 10,0 %	n. a.	3.94E-02	n. a.
The frequency range is indicated for each value to be reported. NOTE Larger tolerances apply for the deviation of the simulation from the reference for frequencies between 0.5 GHz and 0.6 GHz (below cut-off).				

Table 18: XFdtd's results of numerical reflection coefficient evaluation (IEC Table 7) for an YZ orientation and -X propagation direction.

	Limit for code compliance	**TE**		**TM**
axis, direction of propagation and orientation	X, +X, ZY			
ϵ_r		4	4	4
σ [S\m]		0	0.2	0
max. dev. of simulated $Re\{k_{2z}\}$ from numerical reference 1.3 GHz $<$ f $<$ 2 GHz	$\pm$ 5,0 %	4.91E-03	2.51E-02	9.09E-04
max. dev. of simulated $Im\{k_{2z}\}$ from numerical reference 0.5 GHz $<$ f $<$ 0.6 GHz	$\pm$ 5,0 %	n. a.	2.13E-02	n. a.
max. dev. of simulated $Re\{r\}$ from numerical reference 1.3 GHz $<$ f $<$ 2 GHz	$\pm$ 5,0 %	4.86E-03	6.90E-04	3.73E-01
max. dev. of simulated $Im\{r\}$ from numerical reference 1.3 GHz $<$ f $<$ 2 GHz	$\pm$ 5,0 %	n. a.	1.82E-03	n. a.
max. dev. of simulated $Re\{r\}$ from numerical reference 0.5 GHz $<$ f $<$ 0.6 GHz	$\pm$ 10,0 %	3.51E-01	4.69E-02	1.20E-01
max. dev. of simulated $Im\{r\}$ from numerical reference 0.5 GHz $<$ f $<$ 0.6 GHz	$\pm$ 10,0 %	n. a.	3.59E-02	n. a.
The frequency range is indicated for each value to be reported. NOTE Larger tolerances apply for the deviation of the simulation from the reference for frequencies between 0.5 GHz and 0.6 GHz (below cut-off).				

Table 19: XFdtd's results of numerical reflection coefficient evaluation (IEC Table 7) for an ZY orientation and +X propagation direction.

	Limit for code compliance	**TE**		**TM**
axis, direction of propagation and orientation	X, -X, ZY			
ϵ_r		4	4	4
σ [S\m]		0	0.2	0
max. dev. of simulated $Re\{k_{2z}\}$ from numerical reference 1.3 GHz $<$ f $<$ 2 GHz	$\pm$ 5,0 %	4.91E-03	2.51E-02	8.41E-04
max. dev. of simulated $Im\{k_{2z}\}$ from numerical reference 0.5 GHz $<$ f $<$ 0.6 GHz	$\pm$ 5,0 %	n. a.	2.13E-02	n. a.
max. dev. of simulated $Re\{r\}$ from numerical reference 1.3 GHz $<$ f $<$ 2 GHz	$\pm$ 5,0 %	4.86E-03	3.10E-04	3.80E-01
max. dev. of simulated $Im\{r\}$ from numerical reference 1.3 GHz $<$ f $<$ 2 GHz	$\pm$ 5,0 %	n. a.	1.18E-03	n. a.
max. dev. of simulated $Re\{r\}$ from numerical reference 0.5 GHz $<$ f $<$ 0.6 GHz	$\pm$ 10,0 %	3.51E-01	7.49E-02	1.15E-01
max. dev. of simulated $Im\{r\}$ from numerical reference 0.5 GHz $<$ f $<$ 0.6 GHz	$\pm$ 10,0 %	n. a.	1.94E-02	n. a.
The frequency range is indicated for each value to be reported. NOTE Larger tolerances apply for the deviation of the simulation from the reference for frequencies between 0.5 GHz and 0.6 GHz (below cut-off).				

Table 20: XFdtd's results of numerical reflection coefficient evaluation (IEC Table 7) for an YZ orientation and -X propagation direction.

	Limit for code compliance	**TE**		**TM**
axis, direction of propagation and orientation	Y, +Y, XZ			
ϵ_r		4	4	4
σ [S\m]		0	0.2	0
max. dev. of simulated $Re\{k_{2z}\}$ from numerical reference 1.3 GHz $<$ f $<$ 2 GHz	$\pm$ 5,0 %	4.91E-03	2.51E-02	9.09E-04
max. dev. of simulated $Im\{k_{2z}\}$ from numerical reference 0.5 GHz $<$ f $<$ 0.6 GHz	$\pm$ 5,0 %	n. a.	2.13E-02	n. a.
max. dev. of simulated $Re\{r\}$ from numerical reference 1.3 GHz $<$ f $<$ 2 GHz	$\pm$ 5,0 %	4.86E-03	6.90E-04	3.73E-01
max. dev. of simulated $Im\{r\}$ from numerical reference 1.3 GHz $<$ f $<$ 2 GHz	$\pm$ 5,0 %	n. a.	1.82E-03	n. a.
max. dev. of simulated $Re\{r\}$ from numerical reference 0.5 GHz $<$ f $<$ 0.6 GHz	$\pm$ 10,0 %	3.51E-01	4.69E-02	1.20E-01
max. dev. of simulated $Im\{r\}$ from numerical reference 0.5 GHz $<$ f $<$ 0.6 GHz	$\pm$ 10,0 %	n. a.	3.59E-02	n. a.
The frequency range is indicated for each value to be reported. NOTE Larger tolerances apply for the deviation of the simulation from the reference for frequencies between 0.5 GHz and 0.6 GHz (below cut-off).				

Table 21: XFdtd's results of numerical reflection coefficient evaluation (IEC Table 7) for an XZ orientation and +Y propagation direction.

	Limit for code compliance	**TE**		**TM**
axis, direction of propagation and orientation	Y, -Y, XZ			
ϵ_r		4	4	4
σ [S\m]		0	0.2	0
max. dev. of simulated $Re\{k_{2z}\}$ from numerical reference 1.3 GHz $<$ f $<$ 2 GHz	$\pm$ 5,0 %	4.91E-03	2.51E-02	8.41E-04
max. dev. of simulated $Im\{k_{2z}\}$ from numerical reference 0.5 GHz $<$ f $<$ 0.6 GHz	$\pm$ 5,0 %	n. a.	2.13E-02	n. a.
max. dev. of simulated $Re\{r\}$ from numerical reference 1.3 GHz $<$ f $<$ 2 GHz	$\pm$ 5,0 %	4.86E-03	6.90E-04	3.80E-01
max. dev. of simulated $Im\{r\}$ from numerical reference 1.3 GHz $<$ f $<$ 2 GHz	$\pm$ 5,0 %	n. a.	1.82E-03	n. a.
max. dev. of simulated $Re\{r\}$ from numerical reference 0.5 GHz $<$ f $<$ 0.6 GHz	$\pm$ 10,0 %	3.51E-01	4.69E-02	1.15E-01
max. dev. of simulated $Im\{r\}$ from numerical reference 0.5 GHz $<$ f $<$ 0.6 GHz	$\pm$ 10,0 %	n. a.	3.59E-02	n. a.
The frequency range is indicated for each value to be reported. NOTE Larger tolerances apply for the deviation of the simulation from the reference for frequencies between 0.5 GHz and 0.6 GHz (below cut-off).				

Table 22: XFdtd's results of numerical reflection coefficient evaluation (IEC Table 7) for an XZ orientation and -Y propagation direction.

	Limit for code compliance	**TE**		**TM**
axis, direction of propagation and orientation	Y, +Y, ZX			
ϵ_r		4	4	4
σ [S\m]		0	0.2	0
max. dev. of simulated $Re\{k_{2z}\}$ from numerical reference 1.3 GHz $<$ f $<$ 2 GHz	$\pm$ 5,0 %	4.76E-03	2.51E-02	1.37E-03
max. dev. of simulated $Im\{k_{2z}\}$ from numerical reference 0.5 GHz $<$ f $<$ 0.6 GHz	$\pm$ 5,0 %	n. a.	2.12E-02	n. a.
max. dev. of simulated $Re\{r\}$ from numerical reference 1.3 GHz $<$ f $<$ 2 GHz	$\pm$ 5,0 %	4.95E-03	4.92E-04	3.14E-01
max. dev. of simulated $Im\{r\}$ from numerical reference 1.3 GHz $<$ f $<$ 2 GHz	$\pm$ 5,0 %	n. a.	1.60E-03	n. a.
max. dev. of simulated $Re\{r\}$ from numerical reference 0.5 GHz $<$ f $<$ 0.6 GHz	$\pm$ 10,0 %	3.53E-01	4.16E-02	1.12E-01
max. dev. of simulated $Im\{r\}$ from numerical reference 0.5 GHz $<$ f $<$ 0.6 GHz	$\pm$ 10,0 %	n. a.	3.94E-02	n. a.
The frequency range is indicated for each value to be reported. NOTE Larger tolerances apply for the deviation of the simulation from the reference for frequencies between 0.5 GHz and 0.6 GHz (below cut-off).				

Table 23: XFdtd's results of numerical reflection coefficient evaluation (IEC Table 7) for an ZX orientation and +Y propagation direction.

	Limit for code compliance	**TE**		**TM**
axis, direction of propagation and orientation	Y, -Y, ZX			
ϵ_r		4	4	4
σ [S\m]		0	0.2	0
max. dev. of simulated $Re\{k_{2z}\}$ from numerical reference 1.3 GHz $<$ f $<$ 2 GHz	$\pm$ 5,0 %	4.76E-03	2.51E-02	1.29E-03
max. dev. of simulated $Im\{k_{2z}\}$ from numerical reference 0.5 GHz $<$ f $<$ 0.6 GHz	$\pm$ 5,0 %	n. a.	2.12E-02	n. a.
max. dev. of simulated $Re\{r\}$ from numerical reference 1.3 GHz $<$ f $<$ 2 GHz	$\pm$ 5,0 %	4.95E-03	4.92E-04	2.72E-01
max. dev. of simulated $Im\{r\}$ from numerical reference 1.3 GHz $<$ f $<$ 2 GHz	$\pm$ 5,0 %	n. a.	1.60E-03	n. a.
max. dev. of simulated $Re\{r\}$ from numerical reference 0.5 GHz $<$ f $<$ 0.6 GHz	$\pm$ 10,0 %	3.53E-01	4.16E-02	1.15E-01
max. dev. of simulated $Im\{r\}$ from numerical reference 0.5 GHz $<$ f $<$ 0.6 GHz	$\pm$ 10,0 %	n. a.	3.94E-02	n. a.
The frequency range is indicated for each value to be reported. NOTE Larger tolerances apply for the deviation of the simulation from the reference for frequencies between 0.5 GHz and 0.6 GHz (below cut-off).				

Table 24: XFdtd's results of numerical reflection coefficient evaluation (IEC Table 7) for an ZX orientation and -Y propagation direction.

Absorbing Boundary Conditions (ABC) (IEC Section 8.2.3)

The IEC requires two cases–aligned and tilted–in order to validate software compliance with ABC standards. For each case, the results were evaluated and reported for the waveguide oriented along the three axes of the coordinate system, for two different orientations around its axis (rotating the waveguide by 90°), and positive and negative propagation directions along the respective axis. Table 25 lists the 12 orientations. XFdtd's results for the aligned and tilted cases are detailed in the two sections below.

#	Axis	Orientation	Propagation Direction
1	Z	XY	+Z
2	Z	XY	-Z
3	Z	YX	+Z
4	Z	YX	-Z
5	X	YZ	+X
6	X	YZ	-X
7	X	ZY	+X
8	X	ZY	-X
9	Y	XZ	+Y
10	Y	XZ	-Y
11	Y	ZX	+Y
12	Y	ZX	-Y

Table 25: 12 orientations for the ABC tests.

Aligned Absorbing Boundary Conditions (IEC Section 8.2.3.1)

In these tests, a waveguide was truncated into the absorbing boundary of the problem space and the reflection coefficient of the interface was computed. The waveguide was empty (free space) and intersected the outer boundaries perpendicularly. The tests were performed for both TE and TM waves. Both homogeneous and inhomogeneous grids (using the same definitions provided in the Free Space Characteristics section) were tested as well. To meet specifications, the reflection coefficients must fall below -25 dB at frequencies above 1750 MHz, and follow a linear decline between -5 dB at 1370 MHz (10% above cutoff) and -25 dB at 1750 MHz. The permissible power reflection coefficient is shown in Figure 1 below.

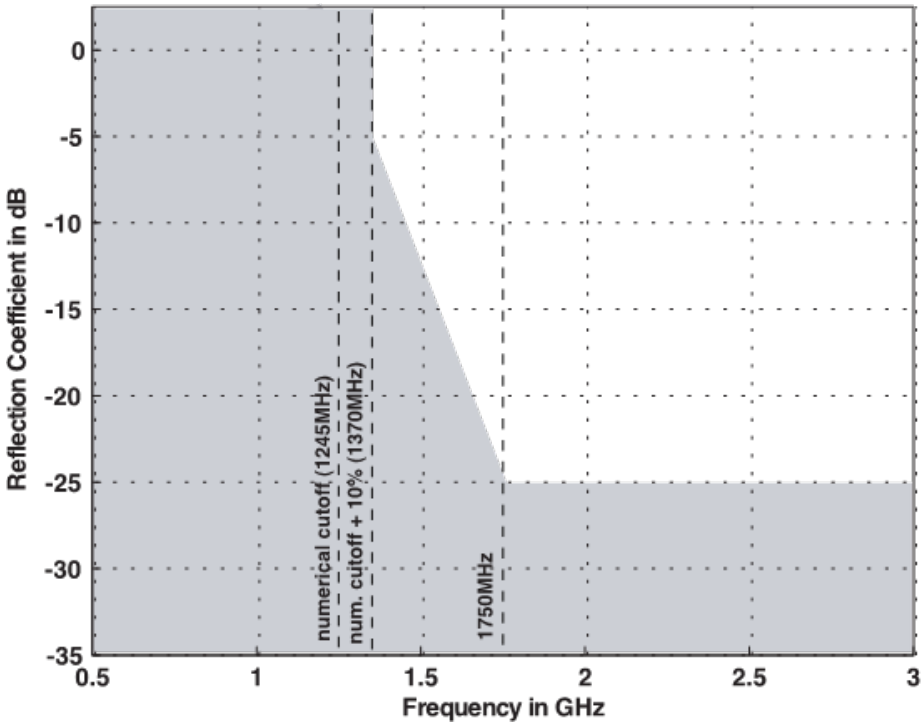

Figure 1: Permissible power reflection coefficient (grey range) with an *aligned* ABC (IEC Figure 7).

The results of the XFdtd tests are summarized in Figures 2–13 that follow. The orientations correspond to Table 25.

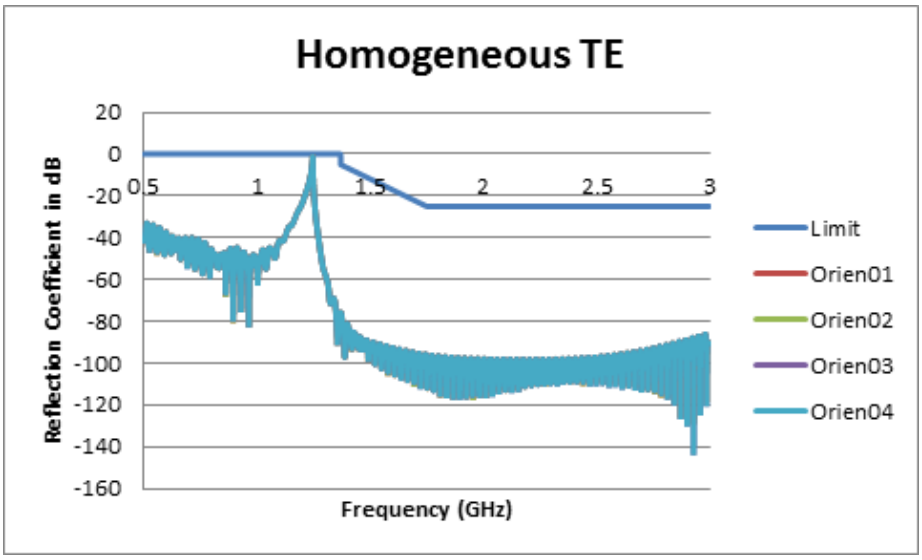

Figure 2: Reflection coefficient computed with XFdtd for the TE homogeneous case (Orientations 1-4) compared to the limit defined in the standard.

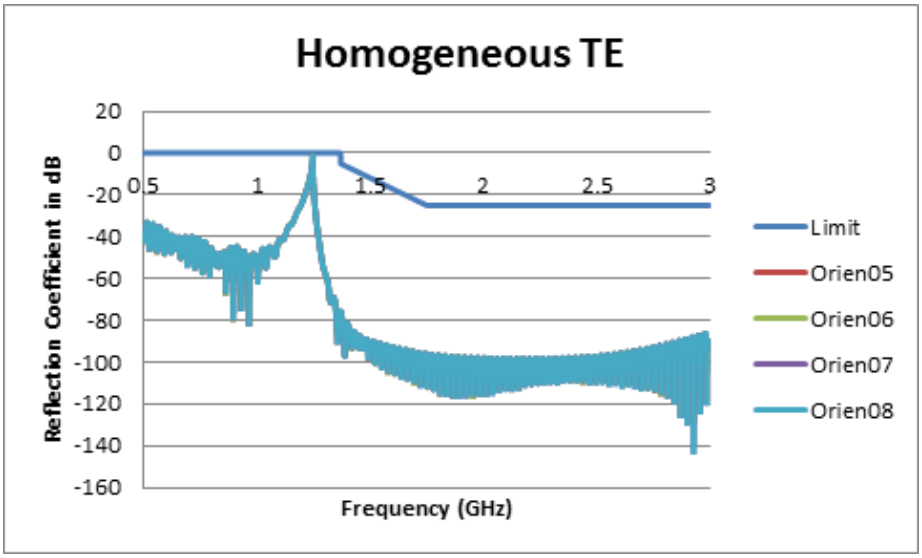

Figure 3: Reflection coefficient computed with XFdtd for the TE homogeneous case (Orientations 5-8) compared to the limit defined in the standard.

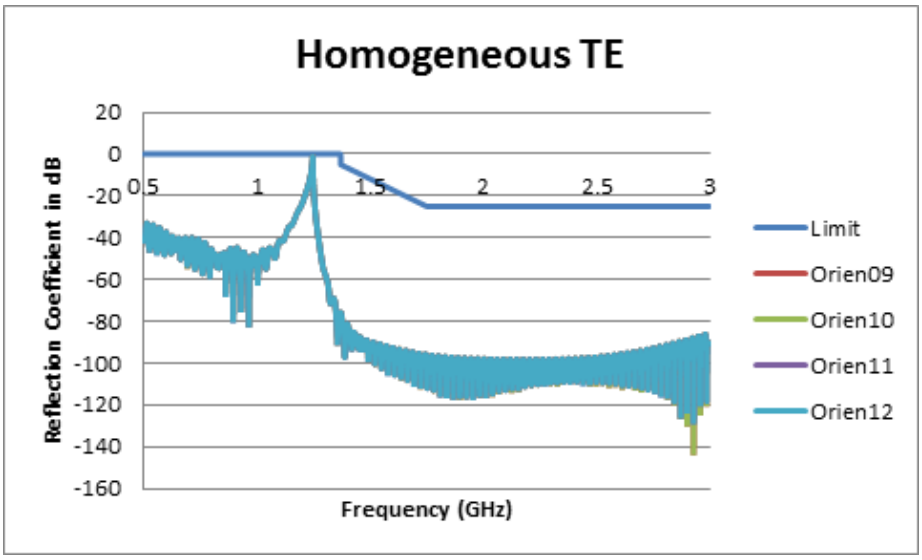

Figure 4: Reflection coefficient computed with XFdtd for the TE homogeneous case (Orientations 9-12) compared to the limit defined in the standard.

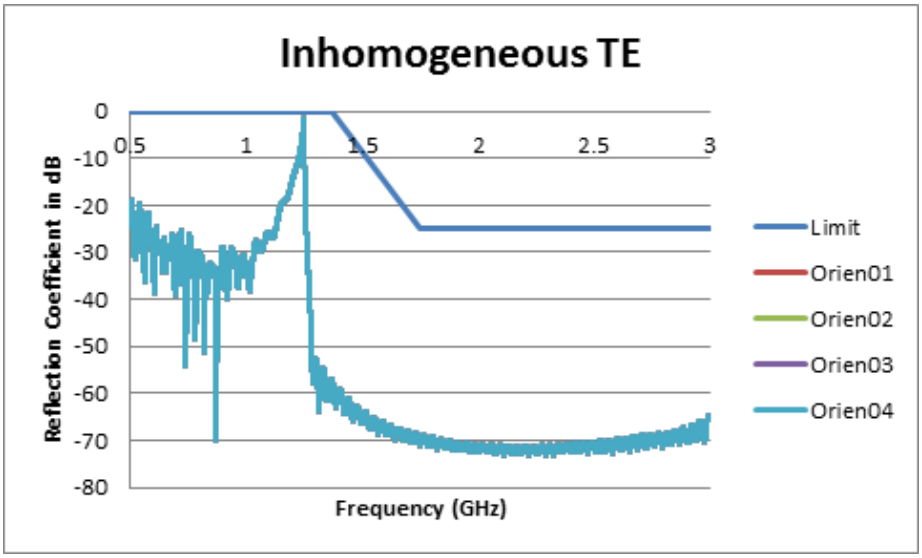

Figure 5: Reflection coefficient computed with XFdtd for the TE inhomogeneous case (Orientations 1-4) compared to the limit defined in the standard.

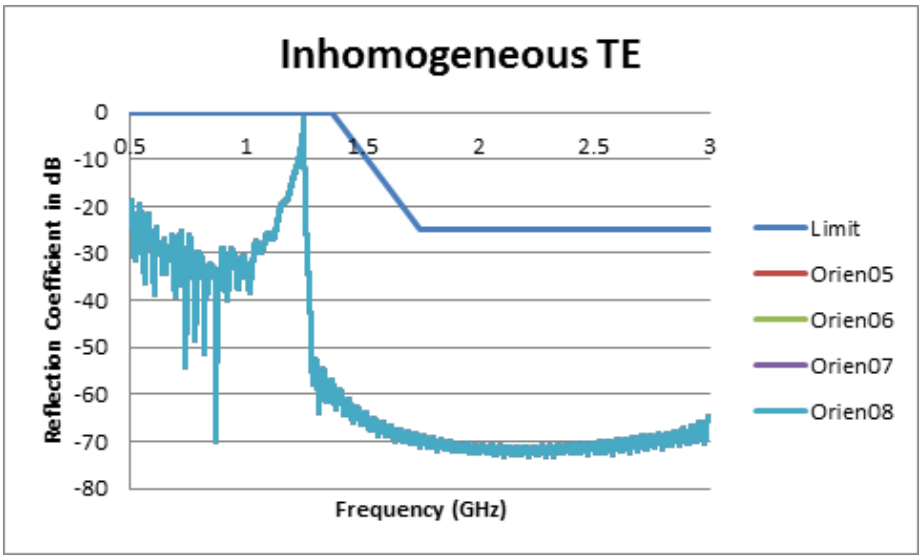

Figure 6: Reflection coefficient computed with XFdtd for the TE inhomogeneous case (Orientations 5-8) compared to the limit defined in the standard.

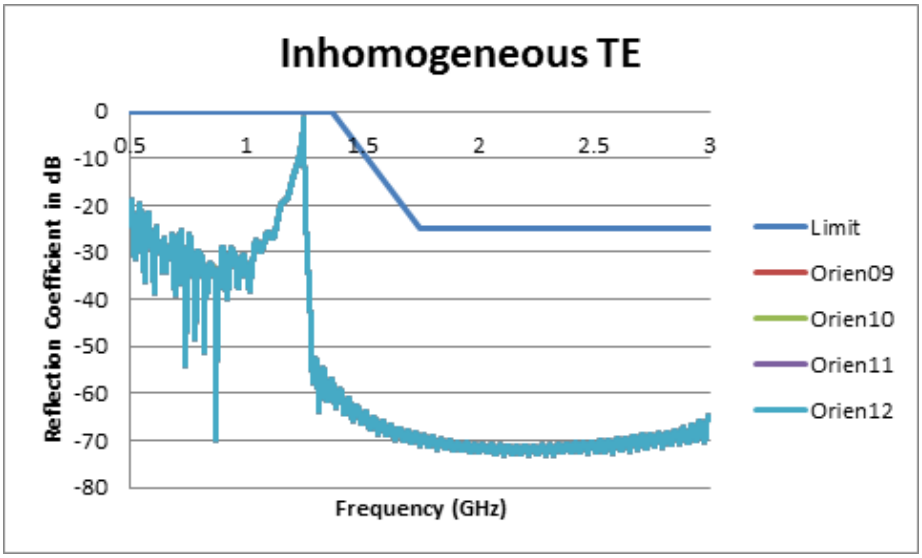

Figure 7: Reflection coefficient computed with XFdtd for the TE inhomogeneous case (Orientations 9-12) compared to the limit defined in the standard.

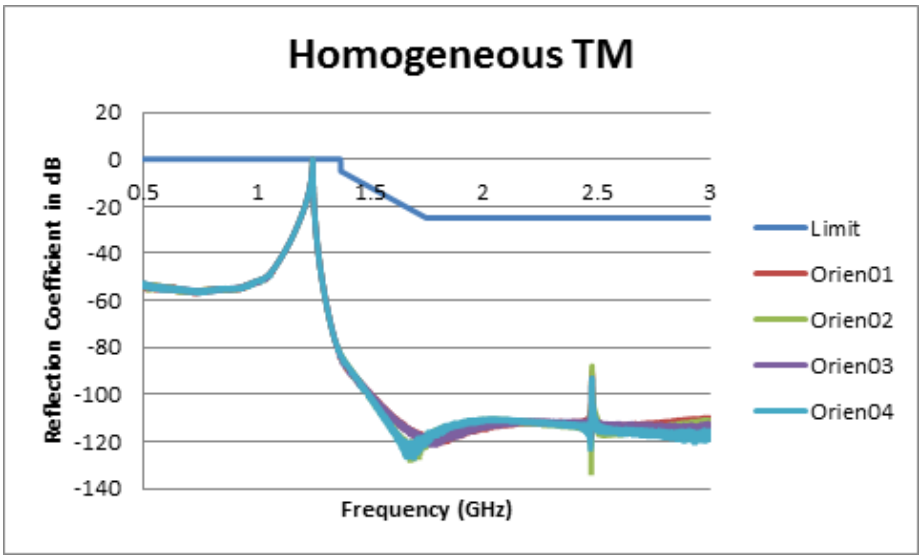

Figure 8: : Reflection coefficient computed with XFdtd for the TM homogeneous case (Orientations 1-4) compared to the limit defined in the standard.

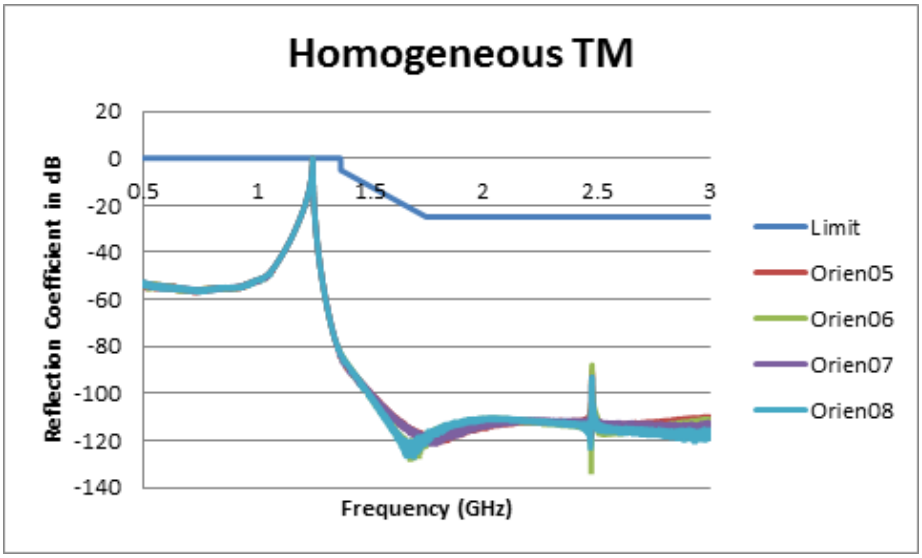

Figure 9: Reflection coefficient computed with XFdtd for the TM homogeneous case (Orientations 5-8) compared to the limit defined in the standard.

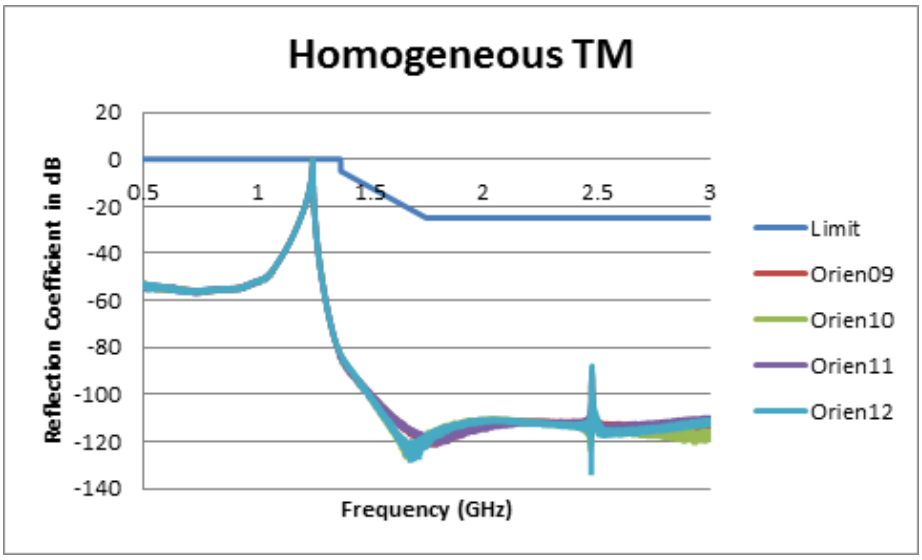

Figure 10: : Reflection coefficient computed with XFdtd for the TM homogeneous case (Orientations 9-12) compared to the limit defined in the standard.

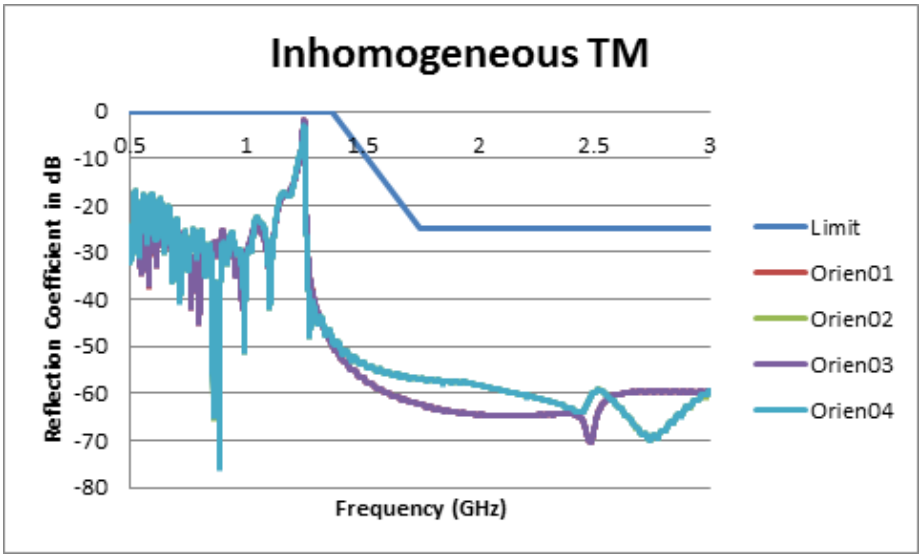

Figure 11: Reflection coefficient computed with XFdtd for the TM inhomogeneous case (Orientations 1-4) compared to the limit defined in the standard.

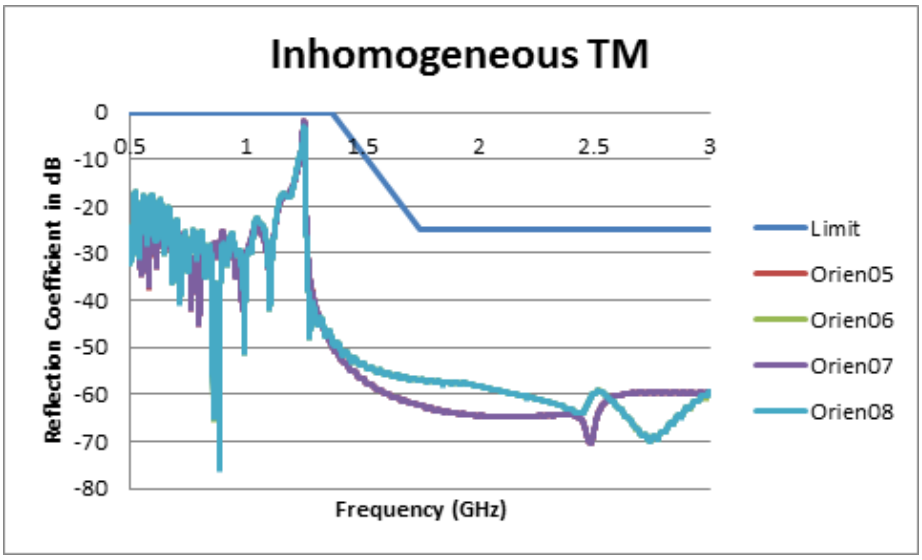

Figure 12: Reflection coefficient computed with XFdtd for the TM inhomogeneous case (Orientations 5-8) compared to the limit defined in the standard.

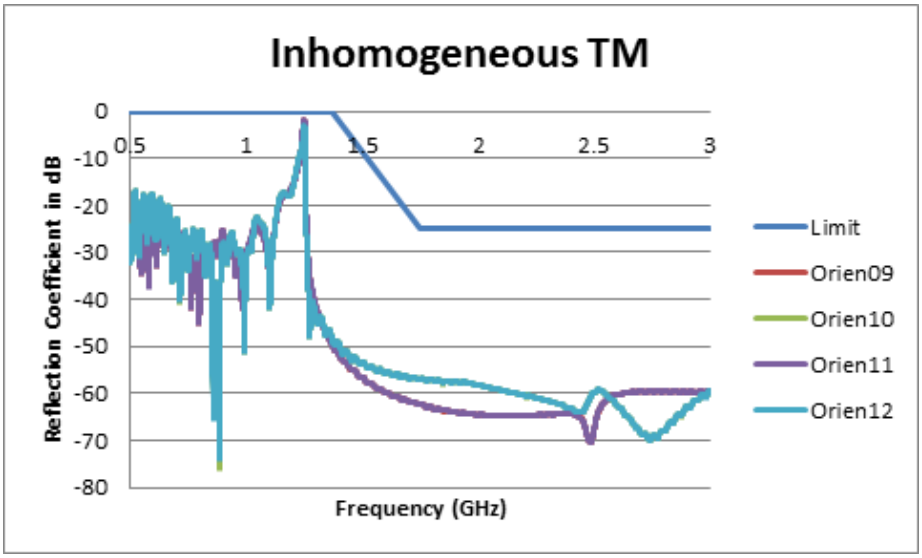

Figure 13: Reflection coefficient computed with XFdtd for the TM inhomogeneous case (Orientations 9-12) compared to the limit defined in the standard.

Performance of the ABCs in the Corners of the Computational Domain (IEC Section 8.2.3.2)

The tests for the reflections from the outer boundary were repeated, but this time for a waveguide terminated into the corners of the FDTD space. The reflection coefficient for the boundary conditions in the corners has to be less than the limits shown in Figure 14.

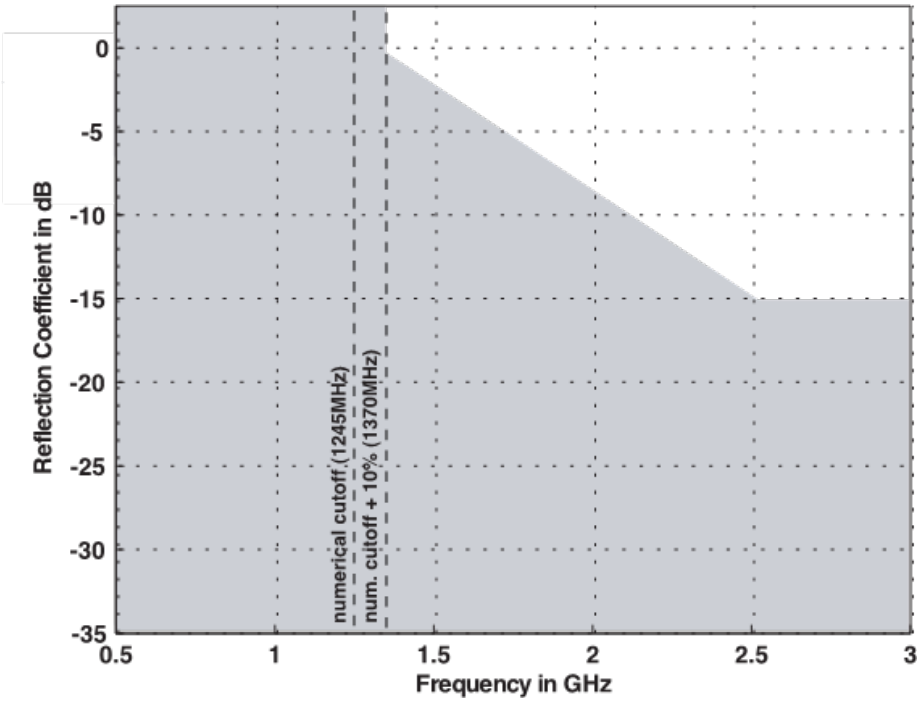

Figure 14: Permissible power reflection coefficient (grey range) with a *tilted* ABC (IEC Figure 9).

The results of the XFdtd tests are summarized in Figures 15–20 that follow. The orientations correspond to Table 25.

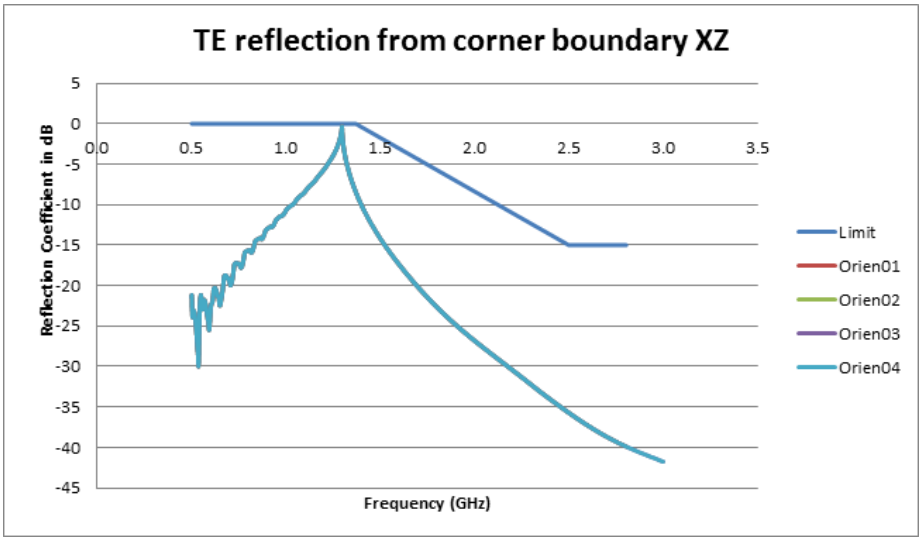

Figure 15: Reflection coefficient results for TE case in XZ plane.

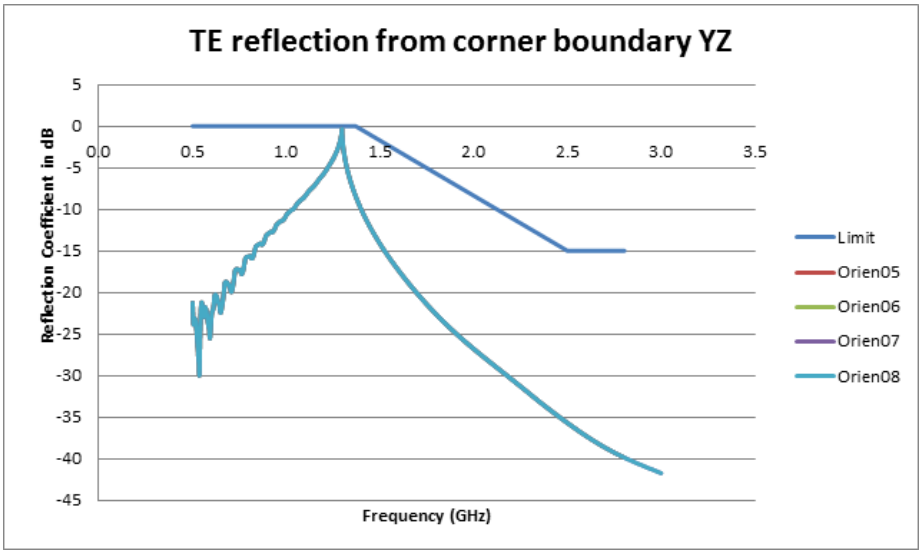

Figure 16: Reflection coefficient results for TE case in YZ plane.

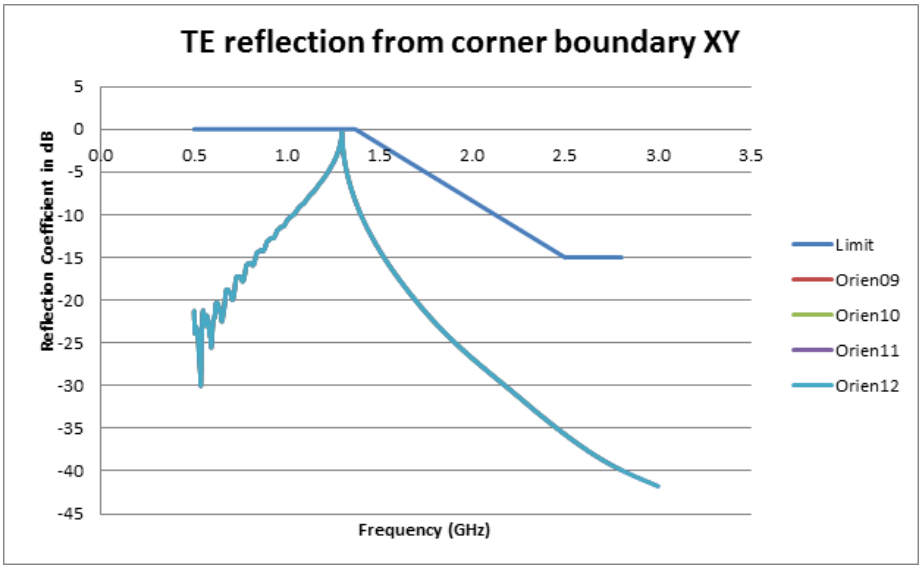

Figure 17: Reflection coefficient results for TE case in XY plane.

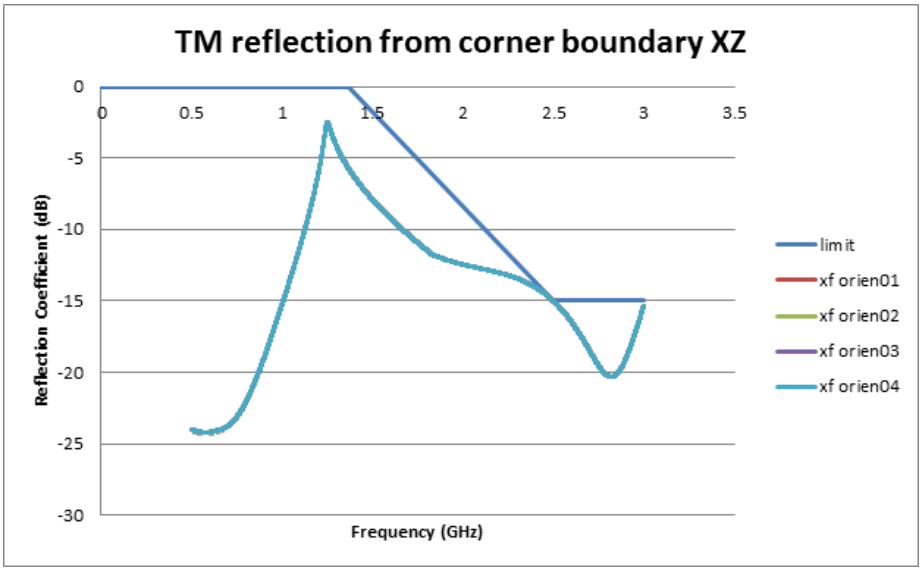

Figure 18: Reflection coefficient results for TM case in XZ plane.

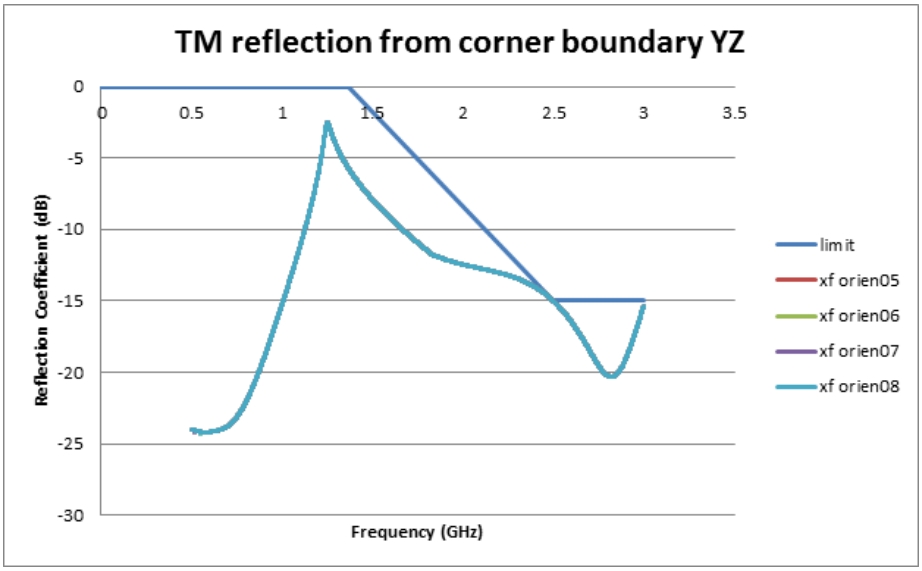

Figure 19: Reflection coefficient results for TM case in YZ plane.

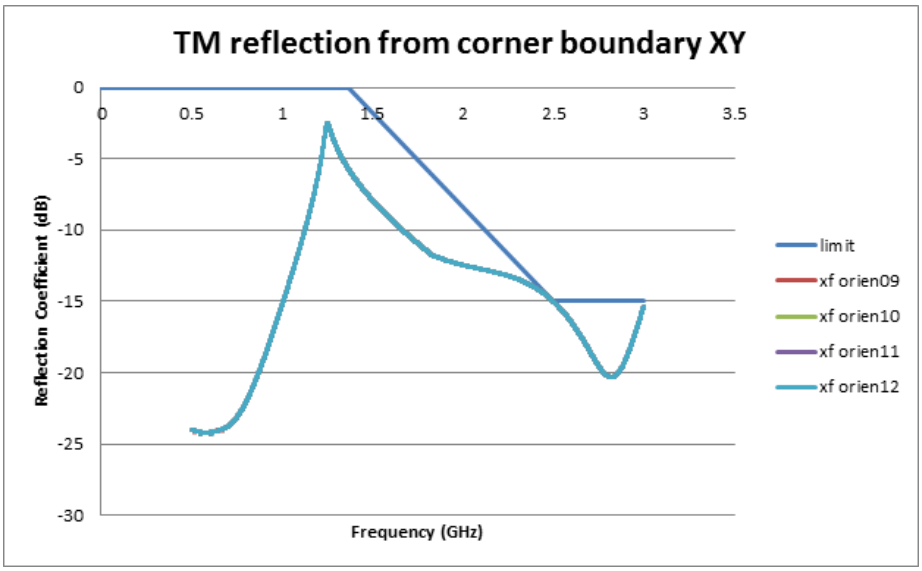

Figure 20: Reflection coefficient results for TM case in XY plane.

SAR Averaging (IEC Section 8.2.4)

XF's averaging algorithm was tested using the SAR-Star geometry with a homogeneous and inhomogeneous mesh. During setup, the models surfaces were aligned with the mesh lines and an incident plane wave was defined. The IEC standard required that certain data be reported, including the status flags that were assigned to each voxel (unused, used, valid, and invalid), the direction into which it has been expanded in case of surface averaging (IEC Section 6.2.2), the dimensions and the mass of the averaged cube that contains the target masses of 1 g and 10 g, the local voxel SAR, and the peak spatial-average SAR assigned to each voxel.

All status flags needed to match the reference results for the algorithm to be validated. The direction into which it is expanded for surface averaging was allowed to differ from the reference results as long as the maximum deviation of the spatial-average SAR in the cube from the maximum value of the six spatial average SAR values of all directions of expansion was within +/- 10% of the reference results. The maximum deviation of the averaging mass and the volume was +/- 0,0002%.

The evaluation script provided in IEC Annex B was run to compare XF's results to the reference results supplied online for the homogeneous and inhomogeneous cases. The evaluation script returned *** ALL TESTS WERE PASSED ***.

Canonical Benchmarks (IEC Section 8.3)

The following benchmark problems were computed to validate XFdtd's compliance with the standard.

Generic Dipole (IEC Section 8.3.1)

The feed-point impedance of a half-wavelength dipole at 1 GHz was evaluated for both broadband and sinusoidal excitations. The dipole had a length of 150 mm and a diameter of 4mm with a 2 mm feed gap in the center. The standard required that broadband simulations save data at 0.5, 1.0, and 1.5 GHz, and that data include impedance and radiated power. XFdtd's data is shown in Table 26 below. All tests passed.

Quantity	Simulation result (Homogeneous mesh)	Simulation result (Inhomogeneous mesh)	Tolerance
$Re\{Z\}$ at 1 GHz	117.137 Ω	110.692 Ω	40 Ω $< Re\{Z\} <$ 140 Ω
$Im\{Z\}$ at 1 GHz	40.875 Ω	46.026 Ω	30 Ω $< Im\{Z\} <$ 130 Ω
Frequency for $Im\{Z\} = 0$	908.398 MHz	909.61 MHz	850 MHz $< f <$ 950 MHz
Power Budget at 0.5 GHz	1.15 %	2.01 %	$<$ 5 %
Power Budget at 1.0 GHz	0 %	0.15 %	$<$ 5 %
Power Budget at 1.50 GHz	0 %	0.17 %	$<$ 5 %
NOTE 1 The tolerances are the deviations which can be expected from a correctly implemented code which has passed the tests defined in IEC Section 8.2. Larger deviations may indicate errors in the modeling or post-processing environment of the code under evaluation.			

Table 26: Results of the dipole evaluation (IEC Table 8).

Microstrip Terminated with ABC (IEC Section 8.3.2)

Data for a microstrip line with a characteristic impedance of 50 ohms on a lossless substrate with relative permittivity of 3.4 was evaluated. The strip width was 2.8 mm and the substrate thickness was 1.2 mm. The geometry was discretized in an inhomogeneous mesh with a maximum cell size of 1 mm and a minimum cell size of 0.1 mm. The microstrip line was excited by a waveguide port and broadband signal covering the frequency range from 0.5 to 2 GHz. The electric fields on the line were saved at three points that were 30 mm apart along the center of the line. The first point was 30 mm from the excitation source. The results are shown in Table 27 below. All tests passed.

Quantity	Reference	Deviation	Tolerance
$Re\{Z\}$	50 Ω	48.66 to 48.73 Ω	45 Ω $< Re\{Z\} <$ 55 Ω
$Im\{Z\}$	0	-0.34 to -0.12 Ω	-2 Ω $< Im\{Z\} <$ 2 Ω
Reflection Coefficient	-∞	Less than -68 dB	$<$ -20 dB

Table 27: Results of the microstrip evaluation (IEC Table 9).

SAR Calculation SAM Phantom/Generic Phone (IEC Section 8.3.3)

The benchmark simulation described in [2] was repeated for the SAM phantom and a generic phone in the touch and tilted positions as described in IEEE 1528 [3] at 835 MHz and 1900 MHz. The 1 g and 10 g peak spatial-average SAR values were reported for the two positions and frequencies. The SAR results were normalized to the feed-point power and the deviation must be less than +/-50% from the reference results reported in [2]. XFdtd's results met the standard as shown below in Tables 28 and 29.

	Reference	XF	Deviation
835 Touch	7.5 W/kg	7.8 W/kg	4.0 %
835 Tilt	4.9 W/kg	5.2 W/kg	5.6 %
1900 Touch	8.3 W/kg	9.3 W/kg	12.1 %
1900 Tilt	12.0 W/kg	12.8 W/kg	7.0 %

Table 28: 1 g results for SAM head simulations.

	Reference	XF	Deviation
835 Touch	5.3 W/kg	5.5 W/kg	4.0 %
835 Tilt	3.4 W/kg	3.4 W/kg	0.5 %
1900 Touch	4.8 W/kg	5.2 W/kg	7.8 %
1900 Tilt	6.8 W/kg	7.2 W/kg	5.2 %

Table 29: 10 g results for SAM head simulations.

Setup for System Performance Check (IEC Section 8.3.4)

The full-sized phantom was evaluated as described in [4] at 900 and 3000 MHz. The maximum cell size used at 900 MHz was 3 mm, resulting in an overall computational domain of 312 x 292 x 213 FDTD cells (480 x 420 x 401.1 mm). The minimum mesh size was 0.225 mm. The SAR and impedance data is shown below in the table. The peak 1 g and 10 g SAR results were within 10% deviation, and the feed point impedance varies by less than 5 ohms as required by the standard. The power budget after adjusting to 1 W of input power has radiated power at 0.13 W and dissipated power at 0.87 W. System efficiency was 12.97% and radiation efficiency was 13.0%. All results met the standard's requirements as shown in Tables 30 and 31.

1 g			**10 g**		
Reference	XF	Deviation	Reference	XF	Deviation
11 W/kg	10.9 W/kg	-0.97 %	7.07 W/kg	7.0 W/kg	-1.43 %

Table 30: Comparison of 1g and 10g results for the flat phantom at 900 MHz.

Resistance			**Reactance**		
Reference	XF	Deviation	Reference	XF	Deviation
49.9 Ω	50.6 Ω	1.45 %	2.3 Ω	5.0 Ω	2.68 Ω

Table 31: Comparison of resistance and reactance results for the flat phantom at 900 MHz.

At 3000 MHz the cell sizes remained the same and the computational domain became 258 x 246 x 166 cells (320 x 280 x 258.8 mm). SAR and impedance data are shown in Table 7. The peak 1 g and 10 g SAR results were within 10% deviation as required by the standard. The power budget, after adjusting to 1 W of input power, had a radiated power of 0.4415 W and a dissipated power of 0.5585 W. System efficiency was 43.88% and radiation efficiency was 43.877%. All results met the standards requirements as shown in Tables 32 and 33.

1 g			**10 g**		
Reference	XF	Deviation	Reference	XF	Deviation
65.4 W/kg	60.6 W/kg	-7.26 %	25.3 W/kg	24.7 W/kg	-2.47 %

Table 32: Comparison of 1g and 10g results for the flat phantom at 3000 MHz.

Resistance			Reactance		
Reference	XF	Deviation	Reference	XF	Deviation
53.4 Ω	57.7 Ω	8.03 %	-4 Ω	-3.4 Ω	0.59 Ω

Table 33: Comparison of resistance and reactance results for the flat phantom at 3000 MHz.

References

[1] International Electrotechnical Commission (IEC) and the Institute of Electrical and Electronics Engineers (IEEE), *IEC/IEEE P62704-1/D4, Determining the Peak Spatial-Average Specific Absorption Rate (SAR) in the Human Body from Wireless Communication Devices, 30 MHz - 6 GHz - Part 1: General requirements for using the Finite-Difference Time-Domain (FDTD) method for SAR calculations*, 2016.

[2] B. B. Beard, W. Kainz, T. Onishi, T. Iyama, S. Watanabe, O. Fujiwara, J. Wang, G. Bit-Babik, A. Faraone, J. Wiart, A. Christ, N. Kuster, A. Lee, H. Kroeze, M. Siegbahn, J. Keshvari, H. Abrishamkar, W. Simon, D. Manteuffel, and N. Nikoloski, "Comparisons of computed mobile phone induced sar in the sam phantom to that in anatomically correct models of the human head," *IEEE Transactions on Electromagnetic Compatibility*, vol. 48, no. 2, pp. 547–558, 2006.

[3] *IEEE Std. 1528-2003, IEEE Recommended Practice for Determining the Peak Spatial-Average Specific Absorption Rate (SAR) in the Human Head from Wireless Communications Devices: Measurement Techniques*.